Single Mutation on the Surface of *Staphylococcus aureus* Sortase A Can Disrupt Its Dimerization†

Jie Zhu, Changsheng Lu,‡ Matthew Standland, Eric Lai, Gabrielle N. Moreno, Aiko Umeda, Xudong Jia,‡ and Zhiwen Zhang*

Division of Medicinal Chemistry, College of Pharmacy, University of Texas at Austin, Austin, Texas 78712

Received July 23, 2007; Revised Manuscript Received November 29, 2007

ABSTRACT: *Staphylococcus aureus* Sortase A (SrtA) is an important Gram-positive membrane enzyme which catalyzes the anchoring of many cell surface proteins conserved with the LPXTG sequence. Recently SrtA has been demonstrated to be a dimer with a K_d of 55 μM *in vitro*. Herein, we show that a single point mutation of amino acid residue on the surface of SrtA can completely disrupt the dimerization. Native polyacrylamide gel electrophoresis and analytical gel filtration chromatography were used to detect the dimer−monomer equilibrium of SrtA mutants. Circular dichroism spectrum experiments were performed to study the conformational change of each SrtA mutant. An enzyme activity assay confirmed that all the SrtA mutants were active *in vitro*. Our results not only are important for understanding the SrtA protein self-associating mechanism but also provided the necessary starting materials for the study of sortase A pathway *in vivo*, which may have significant implications for discovering microbial physiology and give a potential target for novel Gram-positive antibiotics.

Gram-positive bacteria are responsible for eliciting several devastating human diseases, including anthrax, bacteriaemias, pneumonia, tuberculosis, leprosy, and botulism (*1*). By better understanding the mechanism of disease we can develop more effective drugs. The mechanism of virulence in Gram-positive organisms involves cellular adherence of virulence factors via peptidoglycan residues (*2*). These residues exist on a number of cellular membrane anchored proteins, and aid the bacteria in infecting their specific hosts. Many of these virulence factors are initially displayed on bacterial cell wall by the transpeptidase action of sortase proteins (*3*−*6*). Sortase A is a prominent membrane transpeptidase in Gram-positive bacteria. Major threats of diseases such as listeriosis, bacteraemia and pneumonia are direct consequences of the action of sortase A's placement of virulence factors on the cell surface. For example, *Streptococcus gordonii* utilizes SrtA[1] for placement of GspB into the membrane. This protein is involved in adherence to blood platelets during infection (*7*).

It is believed that SrtA catalyzes two sequential reactions via a ping-pong mechanism. The first step is the hydrolysis of the specific sequence LPXTG on primary substrate between the threonine (T) and the glycine (G) to form an acyl-enzyme. The second step is to covalently attach the carboxyl group of threonine to the amino group of glycine from penta-glycine in cell wall bridges through an amide bond resulting in a protein that is linked to the cell wall. It is thought that the first step is the rate-determining step in transpeptidation (*8*).

The currently available crystallography data illustrate sortase A as a monomeric protein with a modified β barrel structure, which is flanked by two short α-helix structures. These monomeric crystals of sortase A have been produced with and without a LPXTG peptide ligand (*9*).

Recently, Lu et al. have shown that $SrtA_{\Delta N59}$ exists as a dimer with a K_d of 55 μM and both the monomer and dimer fractions of the protein were active *in vitro* (*10*). The dimerization between two monomers is highly specific in the context of the entire cellular protein mixture. The exact function of the dimer−monomer equilibrium *in vivo* is not clear yet and currently under study in Zhang lab. It is of interest to understand what physical forces drive the process of dimerization at the molecular level. This understanding of the sortase A mechanism will allow the rational design of molecules which may regulate the extent of dimerization. It has been established in other proteases that catalytic function is dependent on dimerization. For example, the catalytic ability of the Epstein−Barr protease has previously been shown to be dependent on the extent of dimerization (*11*), and HIV-1 protease oligomerization inhibitors are currently in development (*12*).

In an attempt to discover both the location and type of dimerization domain of sortase A, site-directed mutagenesis

† Supported by The Welch Foundation (F1618), American Heart Association (0665198Y), and start-up funds from the College of Pharmacy at The University of Texas at Austin.

* Address correspondence to this author. Division of Medicinal Chemistry, College of Pharmacy, University of Texas at Austin, Austin, Texas 78712, Tel: 512-471-4551. Fax: 512-232-2606. E-mail: zhang@mail.utexas.edu.

‡ Current address: Coordination Chemistry Institute, State Key Laboratory of Coordination Chemistry, Nanjing University, Nanjing, 210093, China.

[1] Abbreviations: SrtA, *Staphylococcus aureus* sortase A transpeptidase; $SrtA_{\Delta N59}$, *Staphylococcus aureus* sortase A transpeptidase without first 59 amino acids on N-terminus; PCR, polymerase chain reaction; FPLC, fast protein liquid chromatography; MS, mass spectrometry; SDS−PAGE, sodium dodecyl sulfate polyacrylamide gel electrophoresis; CD, circular dichroism.

10.1021/bi7014597 CCC: $40.75
Published on Web 01/15/2008

was employed with a rationally chosen host of both hydrophilic and hydrophobic amino acid residues. The generated sortase A mutants were then analyzed for dimerization through their mobility under native conditions on polyacrylamide gel electrophoresis (PAGE), and on a fast protein liquid chromatography (FPLC) size exclusion column. Circular dichroism was carried out to study the effects of mutations on the conformational changes of sortase A. An *in vitro* enzymatic assay was also carried out to ascertain the activity of mutant proteins.

A powerful reduction in dimerization was realized upon replacement of three key hydrophilic residues: N132, K137 and Y143 of which each was mutated to alanyl residues. The generation of new monomeric sortase A mutants paves the way to study the sortase A dimerization *in vivo*. This study is crucial for establishing the true mechanism of sortase A self-association *in vivo*.

MATERIALS AND METHODS

Construction of $SrtA_{\Delta N59}$ and Mutant Protein Expression Vectors. Primers designated PsrtA59 (5′-CGATCCATGGGCCAAGCTAAACCTCAAATTCC-3′) and PsrtA59R (5′-CCGCTCGAGTTTGACTTCTGTAGCTACAA-3′) were used to amplify a $SrtA_{\Delta N59}$ sequence (which would express only residues 60−206) from genomic DNA from *Staphylococcus aureus* subsp. *aureus* (ATCC 700699D) and cloned into the pET28b expression vector to generate the constructs pET28-SrtA59.

The following 11 primers were ordered from Invitrogen for the mutations K62A, I123G, P126G, N132A, K137A, Y143A and K152A respectively.

K62A: 5’ CGA TCC ATG GGC CAA GCT GCA CCT CAA ATT CC 3’

I123G: 5’ GCA GGA CAC ACT TTC GGT GAC CGT CCG AAC TAT 3’ and

5’ ATA GTT CGG ACG GTC ACC GAA AGT GTG TCC TGC 3’

P126G: 5’ ACT TTC ATT GAC CGT GGG AAC TTAT CAA TTT ACA 3’ and

5’ TGT AAA TTG ATA GTT CCC ACG GTC AAT GAA AGT 3’

N132A: 5’ CCG AAC TAT CAA TTT ACA GCT CTT AAA GCA GCC AAA AAA 3` and

5’ TTT TTT GGC TGC TTT AAG AGC TGT AAA TTG ATA GTT CGG 3`

K137A: 5’ CAA CTT TAA AGT ACA CCA TAC TAC CTT TTG CGG CTG CTT TAAG 3’

Y143A: 5’ CAA CTT TAA ATG CCA CCA TAC TAC CTT TTT TG 3’

K152A: 5’GTA CTT TAA AGT TGG TAA TGA AAC ACG TGC GTA TAA AAT G 3’

5’TCA GTG GTG GTG GTG GTG GTG 3’

Site directed mutagenesis for I123G, P126G and N132A was performed as described in the Stratagene protocol (*13*) using pET28-SrtA59 as template plasmid. Mutants K62A, K137A, Y143A and K152A were generated with the following protocol. The DNA fragments containing individual mutagenesis were amplified by polymerase chain reaction (PCR) using forward primer listed above, reverse primer PsrtA59R and pET28-SrtA59 as template plasmid. After double digestion with *Nco*I and *Xho*I, the amplified fragment and pET28-SrtA59 plasmid were then ligated to afford the new mutant vectors (*14*). All plasmids were sequenced to confirm the mutation at their respective site (University of Texas at Austin, ICMB core DNA facility).

Purification of $SrtA_{\Delta N59}$ and Mutant Proteins. The pET28-$SrtA_{\Delta N59}$ and mutant constructs were transformed into *Escherichia coli* strain BL21 (Novagen, La Jolla, CA). The transformed cells were grown in 1 L of Luria broth media at 37 °C until the OD_{600} reached 0.6. The culture was then induced with 1 mM isopropyl β-D-1-thiogalactopyranoside (IPTG, Invitrogen, Carlsbad, CA) and grown for another 6 h at 37 °C. The cells were harvested and incubated on ice for 30 min with lysis buffer (50 mM NaH_2PO_4, 300 mM NaCl, 20 mM imidazole, pH 8.0) containing 1 mg/mL lysozyme. After a brief sonication, the lysate was centrifuged and the supernatant was applied to 0.8 mL of Ni-NTA agarose beads pre-equilibrated with lysis buffer (Qiagen, Madison, WI). After washing off the unbound contaminating proteins, the His6-tagged protein was eluted with elution buffer (50 mM NaH_2PO_4, 300 mM NaCl, 250 mM imidazole, pH 8.0). All samples were analyzed using Coomassie Plus Protein Assay (Pierce Biotechnology, Rockford, IL) measuring the absorbance at wavelength 595 nm to determine the protein concentration.

Native FPLC with Gel Filtration Column. Purified wild type and $SrtA_{\Delta N59}$ mutant proteins were also applied to a Superdex 200 10/300 GL column (Tricorn, Piscataway, NJ) pre-equilibrated in PBS overnight. For each sample, 100 μL of 5 mg/mL sample was injected except for K137A, which had a lower concentration of 2.3 mg/mL. The samples were eluted with washing buffer (0.1 M sodium phosphate, 0.15 M sodium chloride, pH 6.8) at 0.75 mL/min at 4 °C using an AKTA FPLC (Amersham Pharmacia Biotech, Piscataway, NJ). Eluted protein was detected by monitoring at an absorbance of 280 nm. Biomolecules used as molecular weight standards were vitamin B12 (1.35 kDa), horse myoglobin (17 kDa), chicken ovalbumin (44 kDa), bovine γ-globulin (158 kDa), and bovine thyroglobulin (670 kDa), purchased from BioRad (Hercules, CA).

Nondenaturing PAGE. Appropriate dilutions were made for each protein to a total protein concentration of 5 mg/mL prior to analysis by native PAGE using 12% Tris-Glycine gel (Invitrogen, Carlsbad, CA). Approximately 20 μg of each protein was loaded to each lane, along with a NativeMark (Invitrogen, Carlsbad, CA) protein ladder ranging from 20 kDa to 1236 kDa. The gel was visualized by Coomassie Blue staining. For Western blot analyses, proteins were transferred to a nitrocellulose membrane (Hybond-C Extra, Amersham Bioscience, Piscataway, NJ) in a Tris-glycine buffered electrophoresis tank. The membranes were then probed with an anti-His6 C-terminal alkaline phosphatase conjugated antibody (Invitrogen, Carlsbad, CA). The Phospha GLO AP substrate (KPL Incorporation, Baltimore, MD) was applied to visualize the signals, which were detected by exposing the membrane to BioMax Light Film (Eastman Kodak Company, Rochester, NJ). We repeated this experiment three times, as well as at different protein concentrations (data not shown).

Circular Dichroism Spectrum. All the measurements have been repeated three times. Each data point was recorded in triplet. Circular dichroism (CD) studies were conducted with a Jasco J-810 spectropolarimeter (Jasco International Co., Ltd. Tokyo, Japan), and equipped with a Jasco PFD-425S temperature control system. For measurements, all protein

samples were dialyzed against activity assay buffer (50 mM Tris-HCl, 150 mM NaCl, 5 mM $CaCl_2$, pH 7.5) and diluted to a final concentration of 38 μM. CD spectra were recorded from 190 to 250 nm at 25 °C, using a 1 mm cell, a path length of 0.1 nm, a scan rate of 50 nm/min and a response time of 4 s. Spectra were smoothed, and baseline corrected by solvent subtraction before analysis. The recorded spectra in millidegrees of ellipticity (θ) were converted to mean residue ellipticity [θ] in deg·cm^2/dmol·residue by the equation

$$[\theta] = \frac{100\theta M_r}{clN_A}$$

where c is the protein concentration in mg/mL, l is the path length in cm, M_r is the protein molecular weight and N_A is the number of amino acids in the protein. The mean residue molecular weights of 114.4 for wild type SrtA, 114.04 for K62A, K137A and K152A, 114.05 for I123G, 114.15 for P126G, 114.13 for N132A, 113.82 for Y143A were used for calculation. The mean residue ellipticities were then plotted against wavelength by the software KaleidaGraph (version 3.6).

The recorded spectra were also analyzed using the Dichroweb server (*15*). Different algorithms were used for the structure calculations: SELCON3 (*16*), CONTIN (*17*, *18*), and CDSSTR (*19*). Reference data sets 4 and 7 (*15*) were used for our calculations. They contain secondary structure predictions based on ellipticity readings from 190 to 240 nm, which are compatible with our reading wavelength range (*19*). NRMSD parameter was used to evaluate the fitness of various methods (*20*). NRMSD value was calculated as in the equation

$$\mathrm{NRMSD} = \sum[(\theta_{exp} - \theta_{cal})^2/(\theta_{exp})^2]^{1/2}$$

where θ_{exp} is the experimental ellipticities, θ_{cal} is the ellipticities of the back-calculated spectra for the derived structure. A NRMSD value less than 0.1 means that the predicted spectra and the experimental spectra are in close agreement (*21*).

In Vitro Activity Assay. Purified wild type and mutant proteins of sortase A were further studied for their activity. The peptide substrate *o*-aminobenzoyl-LPETG-(2,4-dinitrophenyl)-diaminopropionic acid (Abz-LPETG-Dap(Dnp)) was custom synthesized on PAL resin based on the well-established Fmoc/piperidine strategy (Protein Microanalysis Facility, The University of Texas at Austin). The peptide was cleaved using TFA:water (95/5, v/v) and precipitated using cold diethyl ether. It was then filtered with a fine-porosity fritted glass filter, dissolved in water and lyophilized to dryness. The crude peptide product was purified by HPLC using a preparative C18 column to give ≥90% purity. The peptide Gly_5 was purchased from BACHEM (Torrance, CA). Assays were performed in a volume of 100 μL of assay buffer (50 mM Tris-HCl, 150 mM NaCl, 5 mM $CaCl_2$, pH 7.5) containing 8.4 μM $SrtA_{\Delta N59}$ (or respective mutant proteins), 0.1 mM Abz-LPETG-Dap(Dnp)-NH_2, and 2 mM pentaglycine. Reactions were initiated by the addition of enzyme and incubated at 37 °C for 4 h. Reactions were quenched by the addition of 50 μL of 1 N HCl prior to injection into a reversed-phase C18 fast analytical HPLC column. The peptides of substrate and product were separated using a linear gradient from 10% to 90% CH_3CN/0.1% TFA over 10 min. Dnp-containing peaks were detected by absorbance at 355 nm, and the percentage of reaction product was calculated by integrating the area under the HPLC trace (*22*). To confirm the composition and identity of each product, the peaks were collected and analyzed by MALDI-TOF mass spectrometry and peptide fingerprinting analyses (Analytical Instrumentation Facility Core, The University of Texas).

RESULTS

Expression of Wild Type and Mutant SrtA Proteins. To obtain *S. aureus* SrtA protein for study, the SrtA gene was first cloned and then overexpressed and purified from *E. coli*. A C-terminal His6 tag was used to facilitate the purification of the protein. This His6 tag has been shown to have no effect on SrtA activity (*23*). The full length sortase A is difficult to purify and unstable (*10*). Thus, a truncated SrtA protein ($SrtA_{\Delta N59}$), with the N-terminal 59 amino acids deleted, was generated and purified for further study. The deleted hydrophobic N-terminal region of SrtA functions as a signal peptide for secretion and a stop-transfer signal for membrane anchoring. It is known that $SrtA_{\Delta N59}$ retains the same transpeptidation activity as the full-length SrtA enzyme (*24*, *25*).

The mutant SrtA proteins K62A, I123G, P126G, N132A, K137A, Y143A and K152A were generated by using wild type truncated protein $SrtA_{\Delta N59}$ as a template. Single mutations on specific hydrophilic/hydrophobic amino acid residues were introduced either by using a quick change mutagenesis kit through polymerase chain reaction (PCR) (*13*) or by an established cassette mutagenesis technique (*14*). The expression levels of mutant K62A, I123G, P126G and K152A were comparable with the level of wild type protein. N132A, K137A and Y143A had relatively lower yields, producing only 1/3 to 2/3 of the amount wild type protein can produce.

Gel Filtration Analysis of the Size of Mutant Protein. To determine the size and molecular mass of $SrtA_{\Delta N59}$ mutants, gel filtration experiments with nondenaturing buffer at 4 °C were performed with individual purified proteins(*10*). As shown in Figure 1, elution patterns of all sortase A mutant proteins were aligned with the wild type $SrtA_{\Delta N59}$. The chromatography data indicated that wild type $SrtA_{\Delta N59}$ elutes as three peaks at the concentration of 5 mg/mL (281 μM). The elution volumes on a calibrated Superdex 200 10/300 GL column were used to calculate the molecular mass of each peak. As Figure 1 A black curve shows, for wild type protein, the major peak came out at 15.2 mL and corresponded to the expected dimer species of molecular mass 36,507 Da. The second largest peak corresponding to the expected monomer species came out later at 16.6 mL, and has a molecular mass of 16,766 Da. A minor peak came out earlier at 14.3 mL of molecular mass 59,498 Da, and this peak was deconvoluted to belong to a homo-trimer of $SrtA_{\Delta N59}$. As listed in Table 1, the integrated peak area indicated that the amount of dimer and monomer has a ratio of about 7:1 and the trimer is about the same concentration as monomer. The same pattern was observed for mutant K62A (Figure 1 B blue curve). The dimer of K62A came

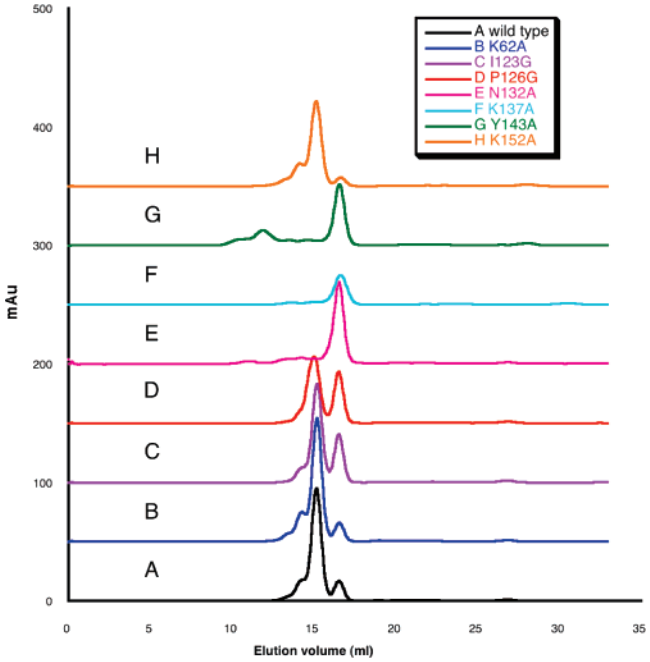

FIGURE 1: Native FPLC with gel filtration chromatography of $SrtA_{\Delta N59}$ and $SrtA_{\Delta N59}$ mutant proteins. Purified wild type and $SrtA_{\Delta N59}$ mutant proteins were applied to a size exclusion gel filtration column. The samples were eluted with washing buffer (0.1 M sodium phosphate, 0.15 M sodium chloride, pH 6.8) at 0.75 mL/min at 4 °C, and the elution pattern was detected by monitoring at an absorbance of 280 nm. Data are overlaid with different colors: A, black, wild type protein; B, blue, K62 → A62; C, purple, I123 → G123; D, red, P126 → G126; E, pink, N132 → A132; F, light blue, K137 → A137; G, green, Y143 → A143; H, orange, K152 → A152.

Table 1: Analytical Size Exclusion FPLC of Wild Type and Mutant $SrtA_{\Delta 59}$ Proteins[a]

	elution volume (mL)		integrated area (mL·mAu)		
	dimer	monomer	dimer	monomer	dimer/ monomer ratio
wild type	15.16	16.53	71.92	10.83	6.77:1.02
K62A	15.19	16.56	75.5076	9.6032	7.86:1
I123G	15.19	16.52	71.159	27.14	2.62:1
P126G	15.01	16.51	56.5573	30.28	1.87:1
N132A		16.52		55.50	
K137A		16.4	1.14	18.29	1:16.0
Y143A		16.47		35.53	
K152A	15.19	16.55	52.0659	4.3159	12.06:1
estimated MW	36507	16766			

[a] Purified wild type and $SrtA_{\Delta N59}$ mutant proteins were applied to a size exclusion gel filtration column. The samples were eluted with washing buffer (0.1 M sodium phosphate, 0.15 M sodium chloride, pH 6.8) at 0.75 mL/min at 4 °C, and the elution pattern was detected by monitoring at an absorbance of 280 nm. The integrated area under each peak was calculated in units of mL·mAu. The relative ratio of peak area was used to estimate the ratio between dimer and monomer species.

out as a major peak and had a 7:1 ratio to monomer peak as shown. This indicated that K62A mutation had no effect on $SrtA_{\Delta N59}$ dimerization.

Significant changes in the elution patterns were observed in mutant I123G (Figure 1 C purple curve) and P126G (Figure 1 D red curve). I123G had the same retention times for dimer and monomer peaks as the wild type $SrtA_{\Delta N59}$ protein, but the integrated dimer to monomer peak area decreased from a 7:1 ratio to a 2.6:1 ratio and the trimer peak was hardly observed from the chromatography. For mutant P126G, two peaks at the same retention volume as wild type $SrtA_{\Delta N59}$ protein gave the integrated dimer to monomer ratio of 1.9:1 and no separate detectable trimer peak was observed. Thus, both of those two mutants at position I123 and P126 showed significantly reduced dimer association of $SrtA_{\Delta N59}$.

Elution patterns from three other mutants, N132A (Figure 1 E pink curve), K137A (Figure 1 F light blue curve) and Y143A (Figure 1 G green curve), indicated almost complete disruption of dimer formation. Both N132A and K137A had a large monomer peak and a very small dimer peak. The dimer-to-monomer ratio of K137A was about 1:16. Mutant Y143A also yielded near complete dimer disruption with a large monomer peak and a hardly detectable dimer peak. However, we also observed that some distinctive peaks eluted before the expected dimer peak. Those peaks corresponded to molecular mass of 190 kDa, 85 kDa and 47 kDa, with a ratio of 10:1:1.5. Fractions from those peaks were collected and subjected to mass spectroscopic analysis. The results indicated that these peaks belong to $SrtA_{\Delta N59}$ oligomers (data not shown).

Although N132A, K137A and Y143A gave upward of 93% disruption of dimerization relative to the wild type dimerization pattern based on gel filtration data, another hydrophilic alanine mutation gave the opposite result. Mutant K152A (Figure 1 H orange curve) had a dimer to monomer ratio of 12:1 in comparison with wild type 7:1. Also, the ratio of trimer to dimer in the K152A mutant was found to be 1:4. Therefore, the trimer:dimer:monomer ratio in this mutant was 3:12:1 compared to the wild type protein of 1:10:1. In this case, enhancement of the $SrtA_{\Delta N59}$ dimerization was achieved.

Based on these data, we successfully generated three mutants which almost completely disrupted the dimerization, N132A, K137A and Y143A; two mutants which reduced the dimerization, I123G and P126G; and interestingly one mutant which increased the dimerization, K152A.

Native PAGE. In contrast to denaturing SDS−PAGE, which resolves proteins mainly on the basis of their molecular mass, the mobility in native PAGE is dictated by both the protein's charge and its hydrodynamic size (*26*). The above $SrtA_{\Delta N59}$ mutants were subjected to the native PAGE analysis (Figure 2). Each lane was loaded with 20 μg of purified $SrtA_{\Delta N59}$ protein at a concentration of 281 μM. This concentration is higher than the previously calculated K_d (55 μM). Since FPLC size exclusion chromatography studies showed that all of the $SrtA_{\Delta N59}$ mutants as well as wild type protein had almost the same molecular mass for the monomer, under this nondenaturing condition, the difference in mobility of major bands is caused by the charges associated with the protein's isoelectric point and/or the overall conformation of the protein which correlates with hydrodynamic size. As seen in Figure 2, compared to wild type protein, K62A, K137A and K152A had higher relative migration velocity during electrophoresis, while Y143A, I123G and P126G did not have significant changes. This pattern can be related to the charges of those proteins at pH 7.4. Based on the calculation from protein calculator (*27*), wild type $SrtA_{\Delta N59}$ had a charge of −0.3, as did I123G, P126G, N132A and Y143A. $SrtA_{\Delta N59}$ mutants K62A, K137A

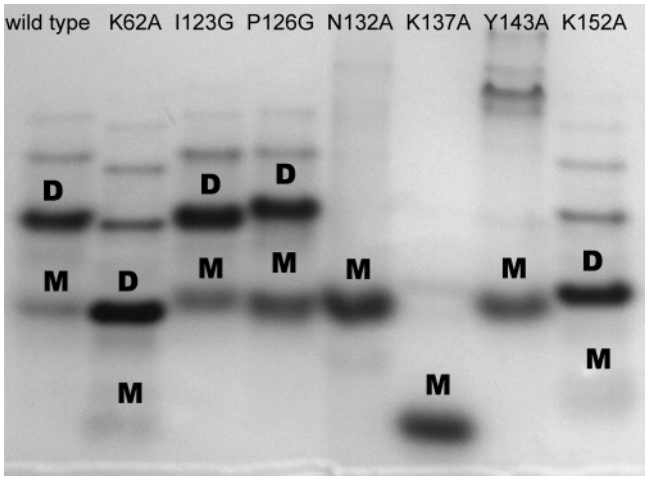

FIGURE 2: Native PAGE of $SrtA_{\Delta N59}$ and $SrtA_{\Delta N59}$ mutant proteins. Purified $SrtA_{\Delta N59}$ and $SrtA_{\Delta N59}$ mutant proteins were first resolved by PAGE under native condition depending on their molecular mass and hydrodynamic size, and then visualized by Coomassie Blue staining. In each lane, 4 μL of 5 mg/mL protein was loaded except for K137A, which has a lower concentration of 2.3 mg/mL. The theoretical mass of a monomer of $SrtA_{\Delta N59}$ is 17.9 kDa, while that of a dimer is 35.8 kDa. The first lane contains $SrtA_{\Delta N59}$ wild type. The lane of K62A contains the mutant $SrtA_{\Delta N59}$ with mutation K62 → A62. The lane of I123G contains the mutant $SrtA_{\Delta N59}$ with mutation I123 → G123. The lane of P126G contains the mutant $SrtA_{\Delta N59}$ with mutation P126 → G126. The lane of N132A contains the mutant $SrtA_{\Delta N59}$ with mutation N132 → A132. The lane of K137A contains the mutant $SrtA_{\Delta N59}$ with mutation K137 → A137. The lane of Y143A contains the mutant $SrtA_{\Delta N59}$ with mutation Y143 → A143. The lane of K152A contains the mutant $SrtA_{\Delta N59}$ with mutation K152 → A152. In each lane, the band labeled on top with D indicates the band of dimeric protein, the band labeled on top with M indicates the band of monomeric protein.

and K152A had a much higher negative charge of −1.3. Since all these proteins had the similar molecular weight, assuming their conformation sizes are the same, the proteins bearing higher negative charges should move faster toward the cathode. The overall conformation of these mutant proteins might not change significantly from the wild type. For instance, monomer band of mutant protein K152A had a slightly lower relative migration velocity compared to the corresponding monomer band of K62A and K137A bearing the same negative charge. The reason could be a slight change in protein folding. A protein with folded chains is more compact than one with partly folded chains. It has relatively smaller size and moves faster in the gel electrophoresis.

The ratios of dimer/monomer of sortase A mutants were estimated by comparing the densities of monomer bands and dimer bands (ImageQuant). The calculated dimer/monomer ratios (D/M) were listed in Table 2. In general, the dimer/monomer ratios estimated from native PAGE are in accord with the measurements from analytical gel filtration FPLC experiments. Several factors may introduce the discrepancy between these two methods, for example, different buffer systems, interaction with different matrix systems, separation time, running temperatures, etc. N132A and Y143A mutations afforded almost complete disruption of sortase A dimer, and K137A mutant had a ratio of dimer/monomer of 1:9.54, which is consistent with data from analytical gel filtration experiments (Table 2). K152A mutation also enhanced the formation of sortase A dimer on a native PAGE (Figure 2), with the ratio of dimer/monomer of 11.6:1 close to that of 12:1 from analytical gel filtration (Table 2). Other three mutants, K62A, I123G and P126G, had small effects on the sortase A dimerization, and their ratios of dimer/monomer were close to that of wild type sortase A on native gel (Figure 2, Table 2), which suggests that these sites are not important for the sortase A dimerization.

The same native PAGE analyses of $SrtA_{\Delta N59}$ mutants were also carried out in different protein concentrations (from 1 mg/mL to 20 mg/mL). Little changes of ratios of dimer/monomer have been observed, particularly N132A, K137A, Y143A and K152A mutants that showed a clearly different pattern than the wild type $SrtA_{\Delta N59}$ (data not shown), suggesting that these $SrtA_{\Delta N59}$ mutants have distinctive dissociation constants.

There are bands with a low mobility for Y143A mutant, besides the monomer band (Figure 2). Mass spectroscopic studies showed that those are the high molecular aggregates of Y143A proteins.

Circular Dichroism Spectrum. To further study the protein folding behavior and the changes of the secondary structure caused by mutagenesis, we performed circular dichroism experiments on wild type $SrtA_{\Delta N59}$ and $SrtA_{\Delta N59}$ mutants. Far UV CD data for $SrtA_{\Delta N59}$ and $SrtA_{\Delta N59}$ mutant proteins in buffer PBS are presented in Figure 3. The recorded spectra in millidegrees of ellipticity (θ) were converted to mean residue ellipticity [θ] in deg·cm^2/dmol·residue. Mean residue ellipticity is the most commonly reported unit, and changes in ellipticity correlate with changes of chirality, which is indicative of changes of secondary structure in proteins. The spectrum of the native protein is characterized by a minimum near 210 nm; $(\theta)_{212.3\ nm} = -9453.86$ deg·cm^2/dmol·residue, and a single positive band near 230 nm; $(\theta)_{232.2\ nm} = 651.90$ deg·cm^2/dmol·residue. A strong negative band near 210 nm could be the combination of disordered polypeptides and α-helix while the small positive band around 230 nm is the feature of β-sheet secondary structure in proteins (*28*). The estimated contents of secondary structure of folded proteins derived from CDSSTR secondary structure method(*19*) using reference data set 4 (*15*) were listed in Table 3. The produced NRMSD fit parameters had very low value ($\ll$0.1), indicating that the calculated secondary structures are consistent with the spectra obtained from experimental measurement. Wild type $SrtA_{\Delta N59}$ contains a combination of mainly β-strand, β-turn and disordered structures, and was estimated by CD to contain 3% α-helix, 45% β-sheet and 21% β-turn and 31% random loop (Table 3). Based on the crystal structure (*9*) and NMR data (*25*) of $SrtA_{\Delta N59}$, among all 145 amino acids, 64 residues are arranged to form β-sheet (44.1%), whereas only 9 residues are involved in α-helix (6.2%), and the remaining 72 residues are connected as turns and structurally disordered loops (49.7%). Therefore, our structural data from CD of wild type protein is in agreement with the NMR data that confirms the validity of our experimental setup. Calculations from individual mutant proteins produced similar secondary structures. By looking at the overlay data of wild type $SrtA_{\Delta N59}$ and mutants in Figure 3, there are no significant changes in β-sheet features, suggesting that there is no gross disruption in the conformation of either protein. All mutants had a peak at 230 nm and a band of negative ellipticity near 210 nm, but the magnitudes were altered in some cases. These differences provided the evidence for

Table 2: Comparison of the Estimation of the Dimer/Monomer Ratios for $SrtA_{\Delta N59}$ Mutants between Native PAGE and FPLC[a]

	WT	K62A	I123G	P126G	N132A	K137A	Y143A	K152A
D/M from PAGE	3.6:1	5.52:1	2.82:1	2.07:1	0	1:9.54	0	11.6:1
D/M from FPLC	6.77:1	7.86:1	2.62:1	1.87:1	0	1:16	0	12.06:1

[a] Purified wild type and $SrtA_{\Delta N59}$ mutant proteins were loaded on native PAGE. The intensities of the protein bands were analyzed using ImageQuant software. The relative ratio of band intensities was used to estimate the ratio between dimer and monomer species (D/M). FPLC data were achieved as described in Table 1.

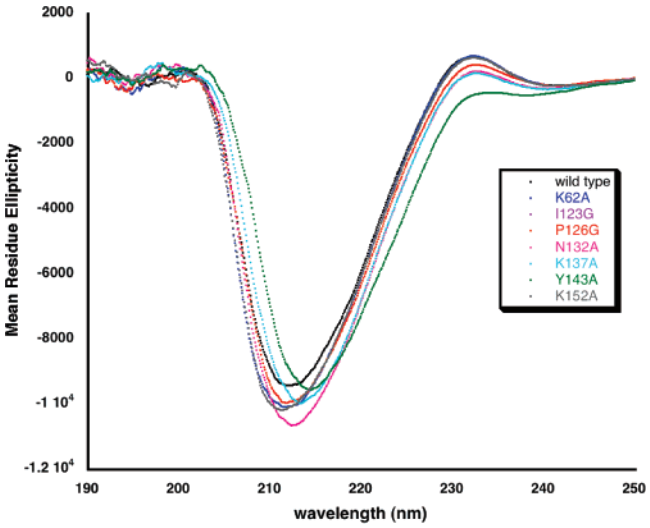

FIGURE 3: Circular dichroism spectrum of $SrtA_{\Delta N59}$ and $SrtA_{\Delta N59}$ mutant proteins. Purified $SrtA_{\Delta N59}$ and $SrtA_{\Delta N59}$ mutant proteins were scanned on circular dichroism spectroscopy. For each sample, 38 μM protein in activity assay buffer was scanned from 190 to 250 nm. Data are overlaid with different colors: black, wild type protein; blue, K62 → A62; purple, I123 → G123; red, P126 → G126; pink, K132 → A132; light blue, Y137 → A137; green, K143 → A143; gray, K152 → A152.

alteration in secondary structure and perhaps the tertiary and quaternary structure (protein−protein interactions) of the mutants by a single amino acid mutation on the protein surface. However, the overall predicted secondary structure content did not change significantly. Consequently, it is clear that none of the mutant structures was radically altered in the sense of producing unfolded proteins as a consequence of the replacement of certain amino acids with alanine or glycine residues in the predicted protein−protein interaction surface area.

In Vitro Activity Assay. To confirm that all the mutant proteins were still active *in vitro*, an activity assay was set up to use Abz-LPETG-Dap(Dnp)-NH_2 as the substrate following the published protocols (*22*). Active sortase A would specifically recognize this LPETG sequence, digest the substrate between T and G and then transfer LPET to the second substrate Gly_5 and release products G-Dap(Dnp)-NH_2 and Abz-LPET-Gly_5. Upon cutting, the released signal of Abz would be recorded at 355 nm by a UV detector and used to calculate the production rate. In a volume of 100 μL reaction system, 8.4 μM of enzyme ($SrtA_{\Delta N59}$ or respective mutant proteins) was incubated with substrates Abz-LPETG-Dap(Dnp)-NH_2 and pentaglycine at 37 °C for 4 h before loaded into an HPLC column. The peptides of substrate and product were separated, and the relative integration areas were used to calculate the conversion ratios. An apparent average velocity during these 4 h was calculated for each protein. Wild type $SrtA_{\Delta N59}$ had an average velocity of approximately 0.03 s^{-1}, and all the other mutant proteins had a similar velocity except for I123G, which had a velocity of 0.01 s^{-1}. This data indicated that all mutant proteins folded in a normal conformation for active sites except for I123G. The possible reason might be that I123 is in close proximity to one of the active site residues H120 (*29*), and that this mutant distorts structures near the active sites. The *in vitro* hydrolysis activity measured by this method at a low concentration less than K_d did not have significant difference in various mutant proteins and wild type $SrtA_{\Delta N59}$, however *in vivo* assays under accurately tailored biological settings would be needed to detect the true differences among dimer disrupted mutants and wild type protein.

DISCUSSION

Based on the experimental data, we tried to identify the roles of specific amino acids in SrtA dimerization. The crystal structure of $SrtA_{\Delta N59}$ by Zong et al. (1T2P) from the Protein Data Bank was analyzed by using Glaxo Smith Kline's DeepView/Swiss-Pdb Viewer. Due to a crystal packing effect, this template crystal has three identical $SrtA_{\Delta N59}$ molecules that originated from three distinct faces of the crystal. The monomer structure of chain B in 1T2P was shown in Figure 4. This template was first characterized based on the amount and type of amino acid residues that protrude from the surface. Then the proximity between different protein subunits among three chains of the $SrtA_{\Delta N59}$ molecule was analyzed. The four top candidate residues based on this methodology were found to be K62, K137, Y143 and K152. Based on the experimental data, K62A did not change the dimerization extent significantly. K152A enhanced the dimerization. However, K137A and Y143A completely disrupted the dimerization and still maintained their correct folding pattern with respect to wild type based on far UV CD data, indicating that these residues are at least partially responsible for self-association of the homodimer. According to the crystal structure 1T2P, Y143 residue on chain A was in a close proximity of 5.57 Å with K137 in chain C, which fits the criteria of cation−π interaction (*30*). Although generally the cation−π interaction has only a moderate energy of about 5 kcal/mol, it is involved in many protein self-associating systems in which the cation−π interaction dictates specificity. One heterodimeric system that involves a cation−π interaction is the cytochrome *c*2/reaction center in *Rhodobacter sphaeroides* (*31*). Site directed mutagenesis studies on this cation−π system by Paddock and associates revealed that replacement of a key tyrosine residue increases the K_d 3-fold (*32*). And in 60% of these cases, the interface with cation−π interaction would have one or more additional cation−anion interactions such as a salt bridge (*33*). This might be able to explain the situation in sortase A. K137 and Y143 on the protein surface are responsible for specificity between the two monomers. After the initial recognition between these two residues, the enthalpically

Table 3: Estimated Secondary Structure Conformation of Mutant and Wild Type of $SrtA_{\Delta 59}$ Proteins[a]

fraction ratio	wild type	K62A	I123G	P126G	N132A	K137A	Y143A	K152A
NRMSD	0.024	0.022	0.022	0.022	0.018	0.019	0.019	0.025
helix:	3%	5%	4%	4%	5%	4%	4%	4%
beta:	45%	45%	50%	50%	50%	47%	46%	47%
turn:	21%	22%	20%	20%	20%	20%	22%	21%
random:	31%	27%	24%	25%	26%	27%	28%	27%
total:	100%	99%	98%	99%	101%	98%	100%	99%

[a] Purified $SrtA_{\Delta N59}$ and $SrtA_{\Delta N59}$ mutant proteins were scanned on circular dichroism spectroscopy. Estimated secondary structure conformation was calculated by Dichroweb server.

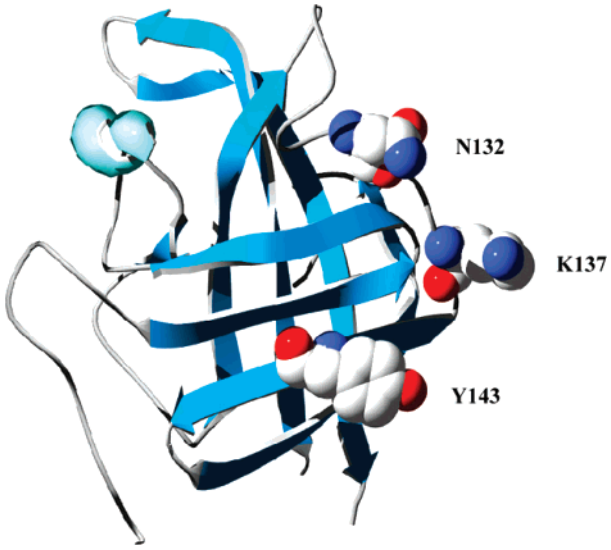

FIGURE 4: Crystallography structure of $SrtA_{\Delta N59}$ wild type proteins. Crystal structure of $SrtA_{\Delta N59}$ wild type proteins (1T2P) from Protein Data Bank was used as template. Chain B was shown here with three key residues labeled. The replacement of each of those three key residues N132, K137 and Y143 with alanyl residue can disrupt sortase A dimerization.

favorable cation$-\pi$ interaction will be formed. The energy from this interaction can be used to rearrange the relative orientations of the two monomers for the residues on the interface to form more hydrogen bonds, electrostatic interactions and hydrophobic interactions, which would give the optimal binding configuration. Mutation on either one of these two residues abolishes the initial recognition and then disrupts the dimerization.

N132A also disrupted 93% of the dimerization with respect to wild type dimer, without much change in folding conformation based on CD data and activity assay. This residue is on the long loop and helix between β4 and β5. It is not on the surface to interact with any other chains in the crystal packing effect structure. Another long loop between β6 and β7 has been demonstrated to be flexible and be able to flip around in regulation of enzyme activity (*34*, *35*). A possible mechanism for N132A dimer disruption might be the loop structure between β4 and β5 has changed such that the dimerization interface is no longer positioned appropriately. This residue is not directly on the surface of interacting domain, however, it determines the correct folding of β5, on which K137 and Y143 both reside, to ensure the recognition of specific residues on interface. N132 might also allosterically control the position of K137. N132's amide oxygen lies 2.8 Å from K134's amide nitrogen, and this hydrogen bond may force K137 into the correct conformation to form the cation$-\pi$ interaction with its Y143 cognate.

In the same manner, the crystal was analyzed for close interactions between hydrophobic surface residues on different chains. There were no close associations found, however, it was found that three hydrophobic amino acids, F122, I123 and P126, shared a close proximity that forms an extending hydrophobic pocket. I123 and P126 were mutated to glycine to exclude any hydrophobic interactions. However, the F122G mutation proved to be difficult to obtain, and only the I123G and P126G mutant proteins were generated. Both of those two mutant proteins demonstrated moderate decrease in dimer formation but not the complete disruption. According to a still debatable theory of protein$-$protein association, the hydrophobic patch on the interface might provide the energy to drive the dimer formation by burial of hydrophobic residues (*36*), and the hydrophilic association among amino acid side chains will determine the specificity between two subunits, and might contribute to complex stabilization as well (*37*). We thus speculate that the mutation on the residue of I123 and/or P126 in this hydrophobic patch can lower the total energy of dimerization and shift the equilibrium toward monomer, but single mutations of either hydrophobic residue are not enough to completely disrupt the homodimer. This explains why a reduced dimer fraction was observed with I123G and P126G mutants but not a complete disruption of the dimer.

CONCLUSIONS

Based on the presented data, three mutant proteins, N132A, K137A and Y143A, were generated that disrupted 93% of the dimerization of $SrtA_{\Delta N59}$, either by directly abolishing the electrostatic interaction between specific residues or by changing the folding process of the protein, leading to incorrectly positioned residues, and an overall decrease of interaction. Further studies with X-ray structures of wild type and mutant proteins will provide new insight into the dimerization of sortase A. Although all the mutant proteins showed similar activity by simple *in vitro* assay, detailed kinetics and *in vivo* activity will be needed in the future to analyze the biological function of sortase A dimerization in *Staphylococcus aureus*.

The current data about the dimerization/oligomerization of sortase A has been obtained *in vitro* and in *E. coli* using a truncated version of sortase A, $SrtA_{\Delta N59}$. We hypothesize that the full-length native sortase A from *Staphylococcus aureus* should behave similarly. The mutants from this study have provided us with the critical starting materials to study the dimerization of native sortase A and its biological effects in *Staphylococcus aureus*.

ACKNOWLEDGMENT

We thank Dr. Katherine Brown for valuable comments on circular dichroism measurement (The University of Texas at Austin). We also appreciate Dr. Stony H. Lo and Dr. Marian Person for their help with mass spectroscopic analyses (The University of Texas at Austin).

REFERENCES

1. Beers, M. H., Berkow, R., Bogin, R. M., Fletcher, A. J., Nace, B. A., Moy, D. E., and Merck Research Laboratories. (1999), Merck, Whitehouse Station, NJ.
2. Boneca, I. G. (2005) The role of peptidoglycan in pathogenesis, *Curr. Opin. Microbiol. 8*, 46−53.
3. Alksne, L. E., and Projan, S. J. (2000) Bacterial virulence as a target for antimicrobial chemotherapy, *Curr. Opin. Biotechnol. 11*, 625−636.
4. Bierne, H., Mazmanian, S. K., Trost, M., Pucciarelli, M. G., Liu, G., Dehoux, P., Jansch, L., Garcia-del Portillo, F., Schneewind, O., and Cossart, P. (2002) Inactivation of the srtA gene in Listeria monocytogenes inhibits anchoring of surface proteins and affects virulence, *Mol. Microbiol. 43*, 869−881.
5. Bolken, T. C., Franke, C. A., Jones, K. F., Zeller, G. O., Jones, C. H., Dutton, E. K., and Hruby, D. E. (2001) Inactivation of the srtA gene in Streptococcus gordonii inhibits cell wall anchoring of surface proteins and decreases in vitro and in vivo adhesion, *Infect. Immun. 69*, 75−80.
6. Mazmanian, S. K., Ton-That, H., and Schneewind, O. (2001) Sortase-catalysed anchoring of surface proteins to the cell wall of Staphylococcus aureus, *Mol. Microbiol. 40*, 1049−1057.
7. Paterson, G. K., and Mitchell, T. J. (2004) The biology of Gram-positive sortase enzymes, *Trends Microbiol. 12*, 89−95.
8. Huang, X., Aulabaugh, A., Ding, W., Kapoor, B., Alksne, L., Tabei, K., and Ellestad, G. (2003) Kinetic mechanism of Staphylococcus aureus sortase SrtA, *Biochemistry 42*, 11307−11315.
9. Zong, Y., Bice, T. W., Ton-That, H., Schneewind, O., and Narayana, S. V. (2004) Crystal structures of Staphylococcus aureus sortase A and its substrate complex, *J. Biol. Chem. 279*, 31383−31389.
10. Lu, C., Zhu, J., Wang, Y., Umeda, A., Cowmeadow, R. B., Lai, E., Moreno, G. N., Person, M. D., and Zhang, Z. (2007) Staphylococcus aureus sortase A exists as a dimeric protein in vitro, *Biochemistry 46*, 9346−9354.
11. Buisson, M., Rivail, L., Hernandez, J. F., Jamin, M., Martinez, J., Ruigrok, R. W., and Burmeister, W. P. (2006) Kinetics, inhibition and oligomerization of Epstein-Barr virus protease, *FEBS Lett. 580*, 6570−6578.
12. Frutos, S., Rodriguez-Mias, R. A., Madurga, S., Collinet, B., Reboud-Ravaux, M., Ludevid, D., and Giralt, E. (2007) Disruption of the HIV-1 protease dimer with interface peptides: structural studies using NMR spectroscopy combined with [2-(13)C]-Trp selective labeling, *Biopolymers 88*, 164−173.
13. Stratagene. QuikChange Site-Directed Mutagenesis Kit Instruction Manual.
14. Kegler-Ebo, D. M., Docktor, C. M., and DiMaio, D. (1994) Codon cassette mutagenesis: a general method to insert or replace individual codons by using universal mutagenic cassettes, *Nucleic Acids Res. 22*, 1593−1599.
15. Lobley, A., Whitmore, L., and Wallace, B. A. (2002) DICHROWEB: an interactive website for the analysis of protein secondary structure from circular dichroism spectra, *Bioinformatics 18*, 211−212.
16. Sreerama, N., and Woody, R. W. (1993) A self-consistent method for the analysis of protein secondary structure from circular dichroism, *Anal. Biochem. 209*, 32−44.
17. Provencher, S. W., and Glockner, J. (1981) Estimation of globular protein secondary structure from circular dichroism, *Biochemistry 20*, 33−37.
18. van Stokkum, I. H., Spoelder, H. J., Bloemendal, M., van Grondelle, R., and Groen, F. C. (1990) Estimation of protein secondary structure and error analysis from circular dichroism spectra, *Anal. Biochem. 191*, 110−118.
19. Sreerama, N., and Woody, R. W. (2000) Estimation of protein secondary structure from circular dichroism spectra: comparison of CONTIN, SELCON, and CDSSTR methods with an expanded reference set, *Anal. Biochem. 287*, 252−260.
20. Mao, D., Wachter, E., and Wallace, B. A. (1982) Folding of the mitochondrial proton adenosinetriphosphatase proteolipid channel in phospholipid vesicles, *Biochemistry 21*, 4960−4968.
21. Brahms, S., and Brahms, J. (1980) Determination of protein secondary structure in solution by vacuum ultraviolet circular dichroism, *J. Mol. Biol. 138*, 149−178.
22. Kruger, R. G., Dostal, P., and McCafferty, D. G. (2004) Development of a high-performance liquid chromatography assay and revision of kinetic parameters for the Staphylococcus aureus sortase transpeptidase SrtA, *Anal. Biochem. 326*, 42−48.
23. Mao, H., Hart, S. A., Schink, A., and Pollok, B. A. (2004) Sortase-mediated protein ligation: a new method for protein engineering, *J. Am. Chem. Soc. 126*, 2670−2671.
24. Ton-That, H., and Schneewind, O. (1999) Anchor structure of staphylococcal surface proteins. IV. Inhibitors of the cell wall sorting reaction, *J. Biol. Chem. 274*, 24316−24320.
25. Ilangovan, U., Ton-That, H., Iwahara, J., Schneewind, O., and Clubb, R. T. (2001) Structure of sortase, the transpeptidase that anchors proteins to the cell wall of Staphylococcus aureus, *Proc. Natl. Acad. Sci. U.S.A. 98*, 6056−6061.
26. Gallagher, Sean R. (1999) in *Current Protocols in Molecular Biology*, Vol. 2 (Ausubel, F. M., Brent, R., Kingston, R. E., Moore, D. D., Seidman, J. G., Smith, J. A., and Struhl, K., Eds.) pp 10.2B.1−10.2B.11, John Wiley & Sons, Inc., New York.
27. Putnam, C. (2006) Protein calculator v3.3.
28. Fasman, G. D. (1996) *Circular dichroism and the conformational analysis of biomolecules*, Plenum Press, New York.
29. Frankel, B. A., Kruger, R. G., Robinson, D. E., Kelleher, N. L., and McCafferty, D. G. (2005) Staphylococcus aureus sortase transpeptidase SrtA: insight into the kinetic mechanism and evidence for a reverse protonation catalytic mechanism, *Biochemistry 44*, 11188−11200.
30. Gallivan, J. P., and Dougherty, D. A. (1999) Cation-pi interactions in structural biology, *Proc. Natl. Acad. Sci. U.S.A. 96*, 9459−9464.
31. Axelrod, H. L., Abresch, E. C., Okamura, M. Y., Yeh, A. P., Rees, D. C., and Feher, G. (2002) X-ray structure determination of the cytochrome c2: reaction center electron transfer complex from Rhodobacter sphaeroides, *J. Mol. Biol. 319*, 501−515.
32. Paddock, M. L., Weber, K. H., Chang, C., and Okamura, M. Y. (2005) Interactions between cytochrome c2 and the photosynthetic reaction center from Rhodobacter sphaeroides: the cation-pi interaction, *Biochemistry 44*, 9619−9625.
33. Crowley, P. B., and Golovin, A. (2005) Cation-pi interactions in protein-protein interfaces, *Proteins 59*, 231−239.
34. Bentley, M. L., Gaweska, H., Kielec, J. M., and McCafferty, D. G. (2007) Engineering the substrate specificity of Staphylococcus aureus Sortase A. The beta6/beta7 loop from SrtB confers NPQTN recognition to SrtA, *J. Biol. Chem. 282*, 6571−6581.
35. Naik, M. T., Suree, N., Ilangovan, U., Liew, C. K., Thieu, W., Campbell, D. O., Clemens, J. J., Jung, M. E., and Clubb, R. T. (2006) Staphylococcus aureus sortase A transpeptidase: Calcium promotes sorting signal binding by altering the mobility and structure of an active loop, *J. Biol. Chem. 281*, 1817−1826.
36. Xu, D., Lin, S. L., and Nussinov, R. (1997) Protein binding versus protein folding: the role of hydrophilic bridges in protein associations, *J. Mol. Biol. 265*, 68−84.
37. Kundrotas, P. J., and Alexov, E. (2006) Electrostatic properties of protein-protein complexes, *Biophys. J. 91*, 1724−1736.

BI7014597